Ferroelectric, conductive, and dielectric properties of $KTiOPO_4$ at low temperature

Q. Jiang, M. N. Womersley, and P. A. Thomas
Department of Physics, University of Warwick, Gibbet Hill Road, Coventry CV4 7AL, United Kingdom

J. P. Rourke
Department of Chemistry, University of Warwick, Gibbet Hill Road, Coventry CV4 7AL, United Kingdom

K. B. Hutton and R. C. C. Ward
Clarendon Laboratory, Parks Rd, Oxford OX1 3PU, United Kingdom

(Received 2 October 2001; published 6 September 2002)

This paper reports the low-temperature dielectric, conducting, and ferroelectric properties of potassium titanyl phosphate, $KTiOPO_4$ (KTP). The change of the dielectric relaxation characteristics as well as the dielectric and conducting properties are related to the decrease of ion hopping frequency with temperature. Between room temperature and 100 K, there are four changes in the behavior of KTP: (i) an increase of K^+ activation energy from 0.25 ± 0.02 eV to 0.40 ± 0.02 eV at 295 K; (ii) a superionic phase transition at ~170 K, accompanied by an increasing thermal absorption and an abnormal change of the thermal expansion; (iii) a phase transition at 140 K associated with the increase of thermal absorption and spontaneous polarization; (iv) a transition from ionic conduction to electronic conduction, which occurs at a frequency-dependent temperature $T_{tr}=-0.3944f^2+12.558f+198.59$ (f in MHz). The conductivity of KTP shows a strong dependence on the electric field and, as a result of this, ideal ferroelectric hysteresis loops cannot be observed. Despite this, the ionic conductivity decreases with temperature sufficiently to allow KTP to be ferroelectrically switched below 250 K. The coercive field is found to take values from 4.4 to 7.0 kV/mm between 250 K to 180 K, respectively.

DOI: 10.1103/PhysRevB.66.094102 PACS number(s): 66.30.Dn

I. INTRODUCTION

Potassium titanyl phosphate (KTiOPO4, KTP) is well-established as a standard nonlinear optical (NLO) crystal for low- and high-power second-harmonic generation (SHG) and optical parametric oscillation (OPO) because of its large NLO coefficients, its use in a noncritical type II phase-matching configuration, its thermal conductivity (~0.03 $W\,cm^{-1}\,°C^{-1}$) and tolerably high damage threshold.[1] To extend the utility of KTP and, in particular, to utilize its largest NLO coefficient, d_{33}, for frequency conversion into the blue and infrared regions of the spectrum, considerable effort has been put into the fabrication of periodically-poled KTP crystals for quasiphase matched (QPM) nonlinear optical interactions.[2–5] In order to enable a ferroelectric switching process that does not damage the crystal, one must avoid or eliminate the effects of the ionic conductivity. The latter results from the combination of quasi-one-dimensional tunnels for potassium migration in the crystal structure and the presence of potassium vacancies in flux-grown KTP crystals.[6] There are currently three methods that enable ferroelectric switching: ion-exchange,[2] Rb-doping of the material during crystal growth,[4,7] and low-temperature poling.[3] In the ion-exchange technique, a thin insulating layer is fabricated at the surface of a crystal by replacing K^+ with Rb^+. When an electric field is applied, there is initially a strong electric field in the near-surface region and a relatively small field in the bulk. Ferroelectrically switched domains are nucleated in the insulating dielectric layer under the periodic electrodes. These domains on both +C and −C sides grow along the **c** direction towards the middle of the crystal, and a periodic pattern of inverted domains results.[2] This method of periodic domain inversion is a two-step process that requires careful operation to avoid thermal cracking of the crystal. Furthermore, the ion-exchange method is prone to the production of optically inhomogeneous crystals because Rb can enter the crystal more rapidly and to a greater depth along the easy diffusion routes formed, for example, by pre-existing defects. To avoid this, in a recent development, an Rb-doped low-conductivity variant of the KTP structure was produced.[4,7] Rb:KTP crystals, with up to 2% Rb substituted for K, were grown from an Rb_2O-containing flux. Conventional ferroelectric switching, as well as periodic poling, was successfully achieved at room temperature without damage to the crystals.[4,7] Using an alternative approach, low-temperature poling of KTP was demonstrated by Rosenman at relatively lower fields[3,8] than that of $LiNbO_3$.

The ionic conductivity of KTP decreases with temperature, as reported by Noda,[9] Rosenman,[8] and Kalesinskas.[10] The latter suspected that there was a superionic phase transition at 280 K since a rather low broad dielectric loss peak was observed at this temperature.[10] On the contrary, Rosenman[3] considered that the superionic phase transition occurs at 140 K, which is consistent with the abnormal increase of the spontaneous polarization, $\mathbf{P}_s$, registered in the pyroelectric coefficient measured by Mangin.[11] However, $\mathbf{P}_s$ as a function of temperature as measured by Shaldin,[12] shows an increase over a wide temperature range (50–150 K). Pisarev[13] shows that the birefringences Δn_{zy}, Δn_{xz}, and Δn_{yx} decrease unusually with temperature below 200 K and a minimum in Δn_{zy} was observed at 140 K. Sheleg[14] shows that the thermal expansion coefficients in the [010] and [001] directions reach a maximum at ~200 K, whereas the coefficient in the [100] direction has a minimum at this tempera-

 ©2002 The American Physical Society

ture. Recent investigations into the ^{31}P nuclear-magnetic-relaxation of KTP have revealed two phase transitions at 200 K and 300 K.[15,16]

The above-mentioned disparate observations contribute to the view that there is an important modification in the properties of KTP at low temperatures, which has relevance to the technological process of periodic poling. Further work is evidently required to clarify these experimental results and to form a consistent picture of the superionic phase transition in KTP. One part of the work involves the investigation of the dielectric relaxation and conducting characteristics at low-temperatures, which are directly related to the hopping of K ions under an alternating electric field. These properties at high temperature have already been investigated extensively,[17] and its isomorph.[18] Furthermore, since a superionic phase transition may often occur over a wide temperature range with accompanying changes in the thermal properties and structural parameters,[19–22] calorimetric, impedance, and thermal expansion measurements were undertaken in this study. The results of these investigations are reported here together with the observation of the change of conducting behavior of KTP from ionic to electronic with both temperature and frequency. In addition, the dependence of the ionic conductivity on the electric field is also shown in order to interpret further the results of Rosenman.[3] Finally, the switching characteristics of KTP are described and the dependence of the coercive electric field on temperature is given.

II. FUNDAMENTAL THEORY

A Cole-Cole plot[23] is often employed to describe the dielectric relaxation of a material with the complex permittivity, ε^*, in the form,

$$\varepsilon^* = \varepsilon' - i\varepsilon'' = \varepsilon_\infty + \frac{\varepsilon_s - \varepsilon_\infty}{1 + (i\omega\tau)^{1-\alpha}}, \tag{1a}$$

where ε_s is the static permittivity and ε_∞ is the permittivity at high frequency, τ is the relaxation time, and α is the angle of the semicircular arc in the plot of ε' and ε''. When $\alpha = 0$, the equation simply describes a Debye-type response[24] and, if the dc conductivity is ignored, the ac conductivity of a material can be written as[24]

$$\sigma(\omega) = A \cdot \frac{\omega^2 \tau}{1 + \omega^2 \tau^2}. \tag{1b}$$

Equation (1a) is empirically-derived and Eq. (1b) has limited application in real solids since it is difficult to observe an ideal Debye response. To understand the ion hopping conduction in a real ionic conductor, different approaches have been used, including the quasi-quantum method of Ishii and Kimball[25,26] and the method of Alexander *et al.*[27] Although both of these methods cannot ultimately model the whole frequency-dispersion of the ionic conductivity in a real material, some general characteristics of ionic conductivity are well described, particularly in the quasi-quantum approach[25] (QQA). In the latter, the ionic motion is regarded as hopping from one configuration (denoted α) to another (denoted γ). If the probability of finding configuration α at time t is $p_\alpha(t)$, the time evolution of the system is governed by the master equation,

$$\frac{\partial p_\alpha(t)}{\partial t} = \sum_\gamma \left[\Gamma^0_{\alpha\gamma} p_\gamma(t) - \Gamma^0_{\gamma\alpha} P_\alpha(t)\right], \tag{2a}$$

where $\Gamma^0_{\alpha\gamma}$ is the transition rate from γ to α and $\Gamma^0_{\gamma\alpha}$ is the transition rate for the reverse process. Since the transition from γ to α is completed by a hop of an ion in configuration α to γ, the functions $\Gamma^0_{\alpha\gamma}$ and $\Gamma^0_{\gamma\alpha}$ can be considered to be ''hopping rates.'' For thermally-induced activation, $\Gamma^0_{\alpha\gamma}$ is proportional to $e^{-(E_a/K_BT)}$ (E_a the activation energy, K_B is the Boltzmann constant). To describe a configuration, the configuration operator R can be introduced,

$$R|\alpha\rangle = R_a|\alpha\rangle. \tag{2b}$$

By assuming there is an equilibrium state, we have a Hermitian operator H, with the symmetric elements as[25,26]

$$H_{\alpha\gamma} = -(\Gamma^0_{\alpha\gamma}\Gamma^0_{\gamma\alpha})^{1/2}, \quad \alpha \neq \gamma = \sum_{\delta\neq\alpha} \Gamma^0_{\delta\alpha}, \quad \alpha = \gamma. \tag{2c}$$

The positive eigenvalues, ε_λ, and the corresponding eigenfunctions, φ_λ, of H can be calculated by setting $\det|H_{\lambda\gamma} - \varepsilon_\lambda \delta_{\lambda\gamma}| = 0$. The eigenfunctions are then the combination of the configurations. The representation of complex ionic conductivity for one-dimensional ionic hopping is given by[25]

$$\sigma^*(\omega) = \frac{1}{K_BT} \cdot \frac{(ze)^2}{V} \cdot \sum_\lambda \langle\phi|R|\varphi_\lambda\rangle^2 \frac{-i\omega\varepsilon_\lambda}{-i\omega + \varepsilon_\lambda}. \tag{3a}$$

Equation (3a) can also be written as

$$\sigma^*(\omega) = \frac{1}{K_BT} \cdot \frac{(ze)^2}{V} \cdot \sum_\lambda \langle\phi|R|\varphi_\lambda\rangle^2 \left[\frac{\omega^2\varepsilon_\lambda}{\omega^2 + \varepsilon_\lambda^2} - i\frac{\omega\varepsilon_\lambda^2}{\omega^2 + \varepsilon_\lambda^2}\right]. \tag{3b}$$

The real part of $\sigma^*(\omega)$ is the conductivity and the complex permittivity is given by [Private communication with Dr. T. Ishii: The $-i$ appears in Eq. (3b) because the relaxation function e^{Ht} rather than e^{-Ht}, was used in the QQA. This results in Eq. (3b) being different from the usual representation of the complex conductivity.]

$$\begin{aligned}\varepsilon^*(\omega) &= \varepsilon_\infty - \sigma^*(\omega)/i\omega \\ &= \varepsilon_\infty + \frac{1}{K_BT} \cdot \frac{(ze)^2}{V} \sum_\lambda \langle\phi|R|\varphi_\lambda\rangle^2 \frac{\varepsilon_\lambda^2}{\omega^2 + \varepsilon_\lambda^2} \\ &\quad + i\frac{1}{K_BT} \cdot \frac{(ze)^2}{V} \cdot \sum_\lambda \langle\phi|R|\varphi_\lambda\rangle^2 \frac{\omega\varepsilon_\lambda}{\omega^2 + \varepsilon_\lambda^2}.\end{aligned} \tag{3c}$$

In at least two cases, the QQA expressions reduce to the representations of the ionic conductivity: (a) when the hopping frequency of all the ions to any vacancies is the same, there are only two eigenvalues; one is the zero corresponding to the ground state ($\varepsilon_1 = 0$) and the other is nonzero ($\varepsilon_2 = \varepsilon$) for the degenerate states. Then, the real part of conductivity is given by

$$\sigma(\omega)=\frac{1}{K_BT}\cdot\frac{(ze)^2}{V}\cdot\frac{1}{\varepsilon_2}\cdot\left[\frac{\omega^2}{\omega^2/\varepsilon_2^2+1}\right]\sum_{\lambda}\langle\phi|R|\varphi_\lambda\rangle^2. \tag{4}$$

Clearly, Eq. (4) is the same as Eq. (1b) or the Debye-function for conductivity and in this case, the dielectric relaxation is the Debye-type. (b) If both the hopping frequencies of ions and the eigenvalues change exponentially, as defined by Ishii,[25] the conductivity can be represented by

$$\sigma^*\propto(-i\omega)^s=\cos\left(\frac{\pi}{2}s\right)\omega^s-i\sin\left(\frac{\pi}{2}s\right)\omega^s, \tag{5}$$

where $0<s<1$.[25] This is appropriate for disordered systems.

Finally, in a simple system, the jumping frequencies of the configurations are proportional to a single thermal activation factor $e^{-(E_a/K_BT)}$. Assuming $\omega\gg\varepsilon_\lambda$, we obtain the Arrhenius equation from Eq. (3b),

$$\sigma(T)=\frac{\sigma_0}{T}\exp\left(-\frac{E_a}{K_BT}\right), \tag{6}$$

where σ_0 is a constant. This equation has been extensively used for modeling the temperature dependence of the ionic conductivity in many materials and for deriving the activation energy, E_a.

III. EXPERIMENTAL METHODS

KTP crystals were grown at Oxford University using the top-seeded solution growth method.[28] The ac conductivity of KTP between 320 K and 120 K was measured using a HP4192A low-frequency impedance analyzer. Silver-coated [001]-cut samples of area 4×4 mm^2 and thickness 0.4 mm were put into a cryostat (Janis Research Company, ST-400). At each temperature, the crystal was left for 15 min to reach thermal equilibrium. The conductivity data at each frequency were gathered via a computer interface established using the HP-Vee software.[29]

Since a superionic phase transition is often accompanied by an exchange of heat with the surroundings or a change of thermal capacitance,[22] the thermal character of KTP was analyzed in the temperature range from 120 to 273 K using a Perkin-Elmer Differential Scanning Calorimeter (model Pyris I). The temperature was ramped at a rate of 10 K/min during both the cooling and heating processes. The thermal expansion coefficient was measured using a purpose-built Kosters-prism optical interferometer capable of measuring changes in thermal expansion coefficient $(1/l)(dl/dT)$ to an estimated accuracy of $\sim6\times10^{-6}$ K^{-1}.[30] A KTP crystal with two [010] faces polished was put into a cryostat (Janis Research Company, ST-100). During the measurement, the temperature was varied continuously from 100 K to 273 K. The electrical response and switching character were investigated using a purpose-built apparatus, which is fully described elsewhere.[31] It is capable of monitoring both the current in the circuit and the dielectric displacement of a crystal. To observe an ideal ferroelectric hysteresis loop, a voltage is applied to compensate the conduction.

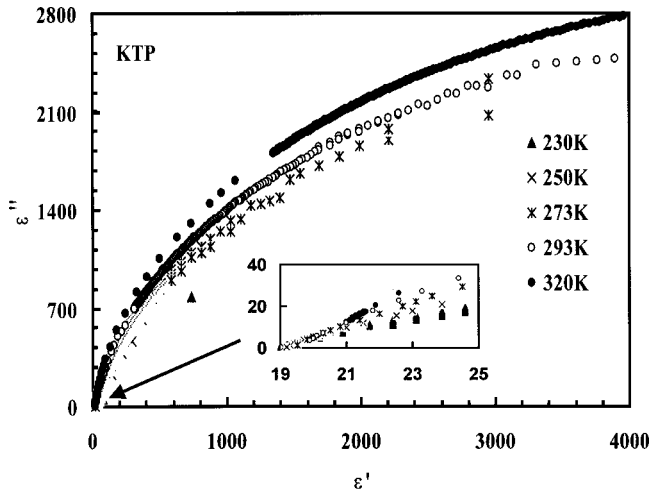

FIG. 1. Cole-Cole plots of KTP at different low temperatures.

IV. RESULTS AND DISCUSSION

A. Dielectric response

The Cole-Cole plots (ε' vs ε'') of KTP at different temperatures are shown in Fig. 1, and the dielectric constant and conductivity as functions of frequency at different temperatures are shown in Figs. 2(a) and 2(b), respectively. It is evident that all of the Cole-Cole plots at different temperatures radiate almost from the same point. This point corresponds to the electronic contribution to the dielectric properties since, as the frequency increases, the coupling between the alternating electric field and the electrons' movement becomes stronger whereas that between the electric field and the movements of ions becomes weaker. As the temperature decreases, the Cole-Cole plots shrink as the result of both a smaller conductivity and a reduced dielectric constant.

Figure 2(a) shows that as the temperature decreases, the decrease of dielectric constant with frequency becomes much more rapid in the low frequency range ($\omega<50$ kHz). This should correspond to a decrease of the eigenvalue, ε_λ, which is the result of the decreased transition rate between the configurations or the hopping rate, since from Eq. (3c), we have

$$\varepsilon'(\omega)=\varepsilon_\infty+\frac{1}{K_BT}\cdot\frac{(ze)^2}{V}\sum_{\lambda}\langle\phi|R|\varphi_\lambda\rangle^2\frac{1}{\omega^2\varepsilon_\lambda^{-2}+1}. \tag{7}$$

The conductivity shown in Fig. 2(b) was fitted well to an equation,

$$\sigma(\omega)=C\cdot\frac{\tau\omega^2}{1+(\tau\omega)^2}\cdot\omega^s, \tag{8}$$

where C, τ, and s are constants at a given temperature. Equation (8) is the combination of Eqs. (4) and (5). When $s=0$, Eq. (8) is the Debye function for the representation of ionic conductivity. When $(\tau\omega)^2\gg1$, it can be written as the real part of Eq. (5). The values for the parameters C, τ, and s for KTP at different temperatures are listed in Table I and their corresponding standard deviations

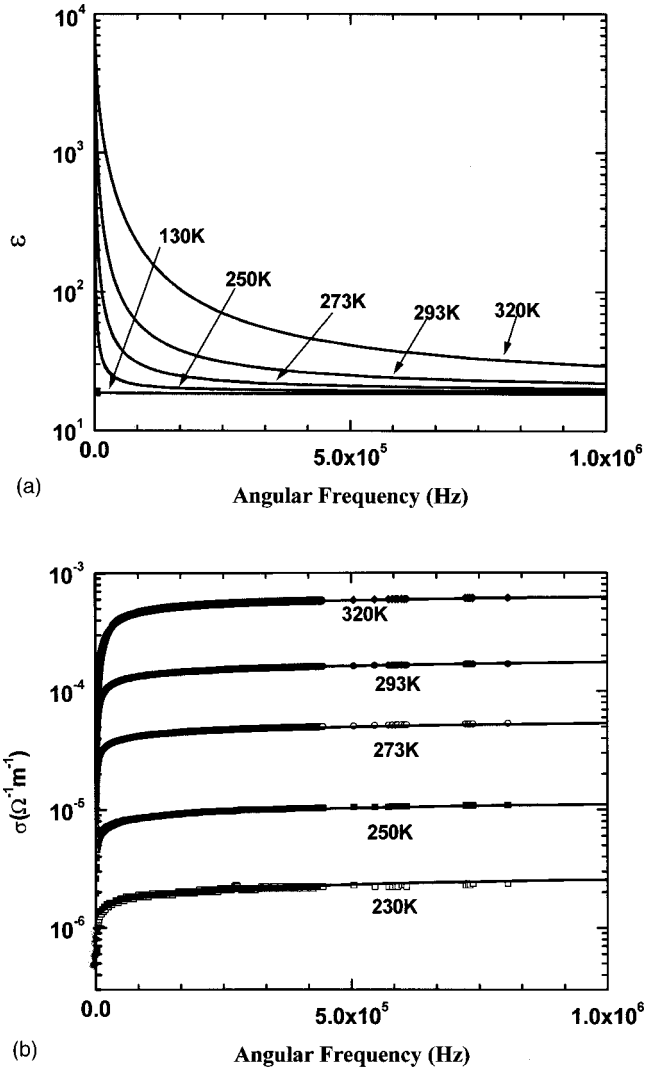

FIG. 2. Dielectric properties of KTP as a function of frequency at different temperatures: (a) Dielectric constant ε_{33} and (b) ionic conductivity along *C*.

$$\Delta\sigma = \frac{1}{n}\sqrt{\sum_{i=1}^{n}\left(\frac{\sigma_i - \sigma(\omega)}{\sigma_i}\right)^2},$$

where n is the number of data points, are $<0.6\%$. The parameter τ increases as the temperature decreases. If Eqs. (7) and (8) are compared, an equivalence of τ and ε_λ^{-1} is suggested. Thus, the decrease of ε_λ, resulting from decreasing temperature, is the reason for both the changes of dielectric constant frequency dispersion and ionic conductivity frequency dispersion. Table I also shows that, the parameter s increases as temperature decreases. This is consistent with the theoretical results obtained by Bernasconi for an one-dimensional disordered system.[32] However, over the temperature range considered here, parameter s is always small compared with unity and the dielectric relaxation is close to Debye-type. This means that a single nonzero engenvalue ε_λ dominates the frequency dispersion of ionic conductivity at each temperature. Therefore, it is appropriate to model the temperature-dependence of the conductivity using Eq. (6).

B. Temperature-dependent conductivity and dielectric properties

The measured dielectric constant and ionic conductivity at different frequencies as a function of temperature are shown in Figs. 3(a) and 3(b), respectively. Both of them decrease with temperature. The Arrhenius plots [Eq. (6) and Figs. 4(a) and 4(c)] clearly show that there are two distinct types of change in gradient occurring between 320 K and 130 K. Type I occurs at low temperature in the low frequency conductivity, e.g., at 185 K for $f=200$ kHz and at higher temperature for high frequency, e.g., at 300 K for $f=10$ MHz. Since increasing the frequency decreases the ionic coupling to the electromagnetic field and increases electronic coupling, the type I gradient anomaly is suggested to be connected with a change in the ratio of ionic conductivity to the electronic conductivity. Using the flat part of the curve at 10 MHz in Fig. 4(a) and supposing the electronic conductivity is proportional to $e^{-(E_e/K_BT)}$ (E_e is the activation energy of electrons), we can estimate the electron activation energy to be ~ 0.04 eV, which is about 10% of the activation energy for ionic conductivity. Therefore, the ionic conductivity decreases much more rapidly than the electronic conductivity with temperature and at a critical temperature (T_c) the ionic conductivity becomes less than the electronic conductivity. At higher frequency, the electronic conductivity will exceed the ionic conductivity at higher temperature, as shown in Fig. 4(a), since the electron-electromagnetic wave coupling is stronger. By extending the flat lines of the lower temperature range [e.g., large value of $(K_BT)^{-1}$] of the Arrhenius plots to room temperature, the electronic conductivity at different frequencies at room temperature can be estimated with an error $<3\%$. The experimentally-derived ratios of ionic to electronic conductivities for three frequencies at room temperature are listed in Table II. Evidently, both types of conductivity increase with frequency, but the electronic conductivity increases more rapidly, as expected. The critical temperature at a function of frequency is drawn in Fig. 4(b), which shows that the dielectric constant and conductivity variations with frequency are of the ionic conducting origin, as discussed. Similar ionic to electronic conduction transitions were also observed by Urenski *et al.*[33,34] However,

TABLE I. Parameters for the representation of ionic conductivity of KTP at low temperatures.

Temperature (K)	320	293	273	250	230
S	0.098	0.100	0.105	0.110	0.14
$\tau(s)$	7.0×10^{-5}	2.0×10^{-4}	5.2×10^{-4}	9.8×10^{-4}	1.4×10^{-3}
C	1.18×10^{-8}	8.82×10^{-9}	6.53×10^{-9}	2.38×10^{-9}	5.25×10^{-10}

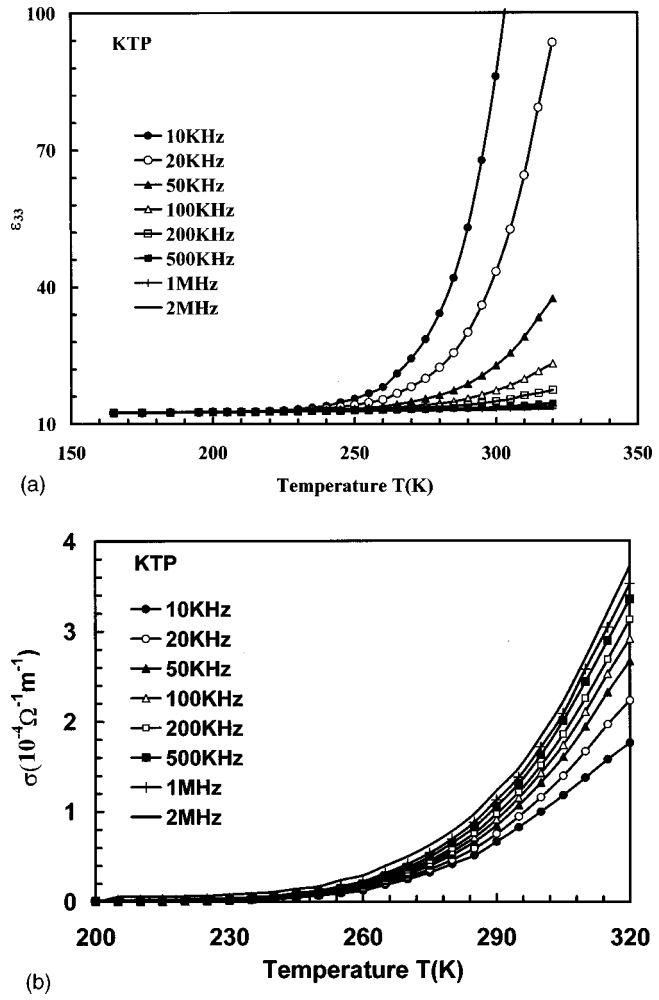

FIG. 3. Dielectric properties of KTP as a function of temperature at different frequencies: (a) Dielectric constant ε_{33} and (b) ionic conductivity along *C*.

since their investigations were carried out at single frequency, the physical mechanisms for such a transition cannot be clarified, i.e., whether such a transition is caused by a superionic phase transition or the electromagnetic field interaction with an ionic conductor.

The type II gradient anomaly, which signifies a change in activation energy from 0.25 eV to 0.40 eV, occurs between 250 K and 305 K $[(K_BT)^{-1}$ from 43 to 38] and is clearly shown in Fig. 4(c). This anomaly corresponds to a quickening of the rate of decrease in the ionic conductivity with decreasing temperature. Within this temperature range, an abnormal change in the dielectric loss was observed by Kalesinskas[10] and he concluded that the superionic phase transition occurred at 268 K. However, such an anomaly might equally well be caused by an order–disorder transition[22] and has been interpreted as a change of the conduction mechanism from polarons (K^+ + lattice deformation) to K^+ alone.[15] To clarify this, the results of the thermal analysis must be considered.

C. Thermal absorption and thermal expansion

The thermal absorption spectrum is shown in Fig. 5(a). An absorption peak was observed at 180 K on repeated heat-

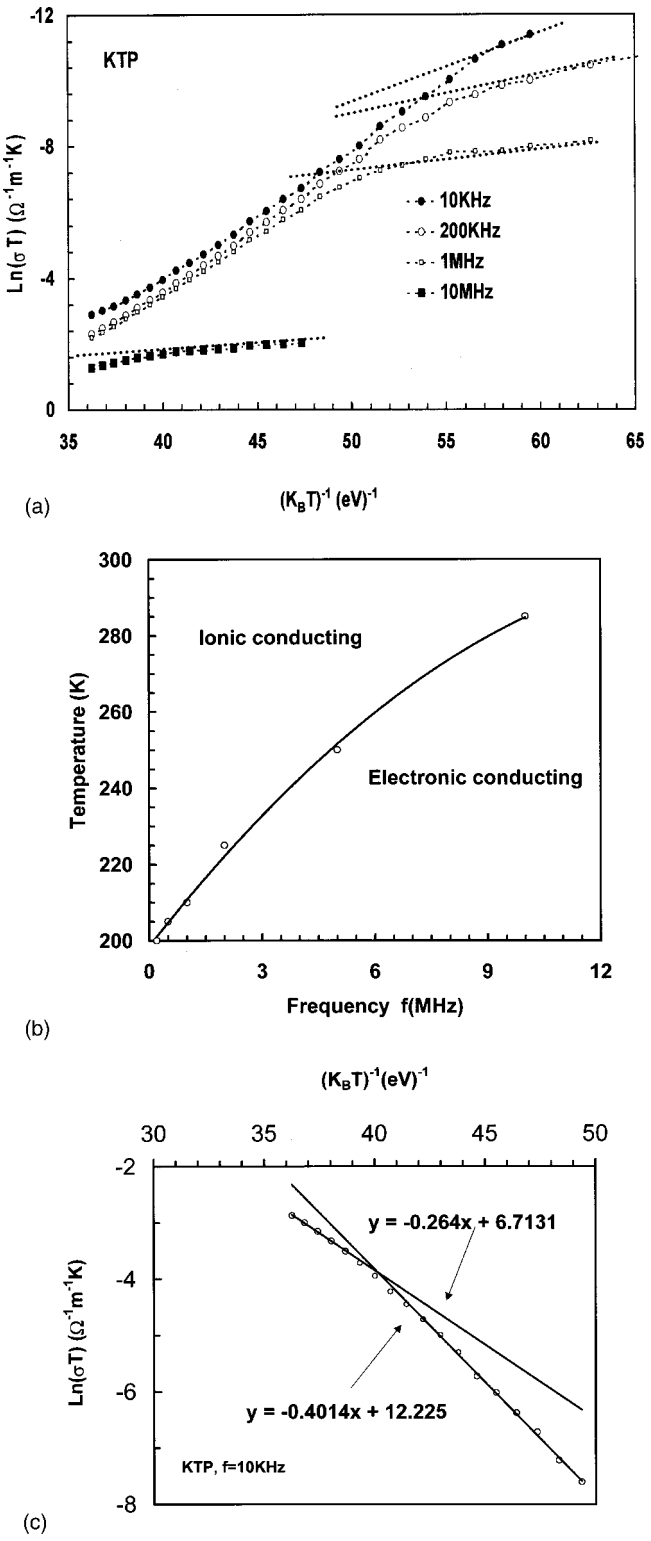

FIG. 4. (a) Parameter $\ln(\sigma T)$ as a function of parameter $(K_BT)^{-1}$. The dotted lines show the supposed curves corresponding to the electronic conductivity. (b) The dependence of the conducting mechanism in KTP on both the frequency and temperature. (c) Parameter $\ln(\sigma T)$ as a function of parameter $(K_BT)^{-1}$ between 250–320 K, showing that the activation energy increases from 0.26 eV to 0.40 eV at 290 K.

TABLE II. Comparison of ionic conductivity and electronic conductivity at room temperature.

	200 KHz	1 MHz	10 MHz
$\sigma_{ion}(\Omega^{-1}\,m^{-1})$	9.75×10^{-5}	1.13×10^{-4}	4.05×10^{-4}
$\sigma_{electron}(\Omega^{-1}\,m^{-1})$	3.62×10^{-7}	1.41×10^{-5}	2.39×10^{-4}
$\sigma_{ion}/\sigma_{electron}$	269	80	1.7

ing, whereas a broad peak on cooling was observed at ~165 K. The difference in temperature on heating and cooling is attributed to thermal hysteresis in the phase transition temperature. Despite the apparent differences in the peak-shapes, all three peaks extend over ~40 K when compared with the baseline. This is characteristic of a superionic phase transition. The variation of the thermal expansion along [010] with temperature [Fig. 5(b)] shows an abnormality in a similar temperature range, and resembles the results obtained using x-ray diffraction by Sheleg.[14] It is not possible to gain direct evidence for the superionic phase transition below 180 K because of the small ionic conductivity and the resolution of our impedance analyzer. For example, the Arrhenius plot of 10 kHz in Fig. 4(a) shows that the electronic-ionic critical temperature is at $Tc=200$ K, whereas the superionic phase transition should be below this temperature. However, below this temperature, the change of ionic conductivity is beyond the resolution of the impedance analyser. Nevertheless, in comparing these data with other literature,[20–22] we suggest that the superionic phase transition occurs near 180 K and the increase in activation energy at 270 K, which was thought to be a superionic phase transition by Kalesinskas,[10] is the result of an order–disorder transition.[22]

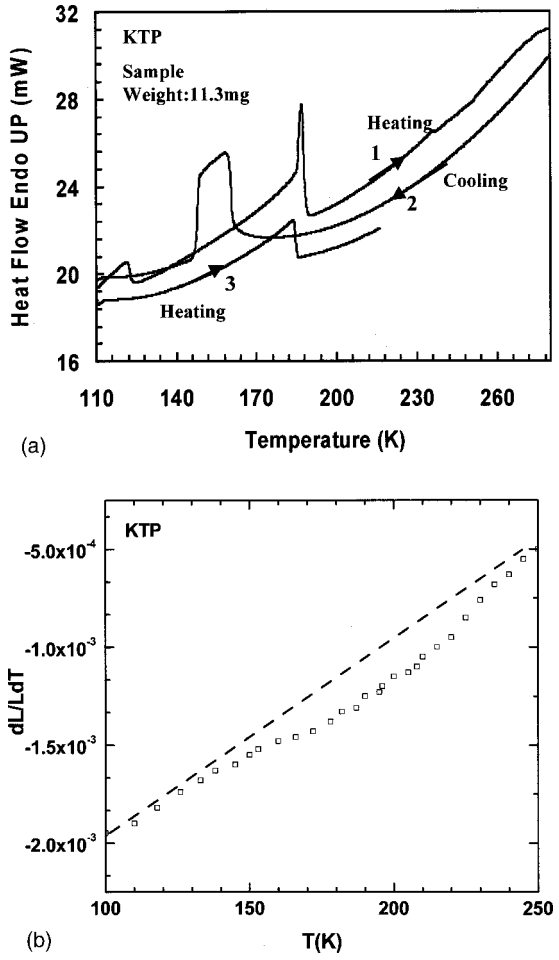

FIG. 5. (a) Heat absorption peaks of KTP at low temperatures. Line 1 shows the heat absorbed when the sample was heated from 110 K to 280 K. Line 2 shows that in the subsequent cooling process and line 3 shows the repeated heating process. (b) Measured thermal expansion of KTP at low temperatures. The dots are the measured data point and the dashed line represents the expected thermal expansion coefficient without a superionic phase transition.

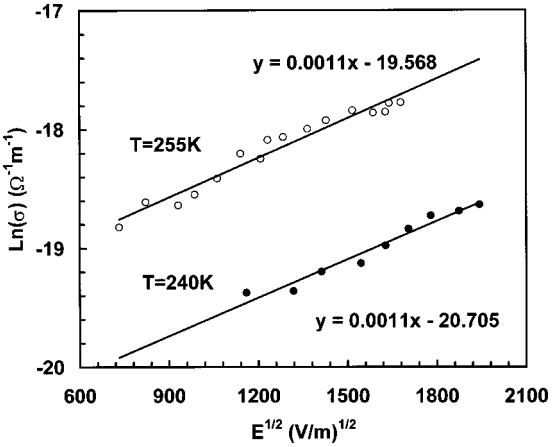

FIG. 6. Dependence of ionic conductivity of KTP on electric field as the results of Poole-Frenkel effect. The empty and filled dots represent the value of $\ln(\sigma)$ that depends linearly on $E^{1/2}$, as shown by the solid fitting lines.

There is also a small thermal absorption peak on cooling near 120 K. Taking into account the thermal hysteresis, this would occur at 140 K on heating. At this temperature, an abnormal increase in the spontaneous polarization was observed by Shaldin[12] and by Mangin.[11]

D. Poole-Frenkel effect in KTP crystals

When a dielectric is subject to an electric field, its dc conductivity increases with the field in the form,[35]

$$\sigma=\sigma_1 e^{(e^3E/\varepsilon\varepsilon_0)^{1/2}/K_BT}, \tag{9}$$

where ε is the high-frequency dielectric constant and σ_1 represents the field-independent component of the conductivity. Figure 6 shows that $\ln(\sigma)$ for KTP depends linearly on the square root of the dc electric field at temperatures of 255 K and 240 K. The high frequency dielectric constant derived from these plots is 19.0 ± 0.5, of a similar order to the value of 15.0 ± 0.3 measured at 10 MHz and 255 K. The field-dependence of the conductivity is consistent with a standard Poole-Frenkel effect.[35] In order to evaluate if the conductivity decreases with temperature, Eq. (9a) is combined with Eq. (6a), and the dc conductivity of KTP is represented as a function of both electric field and temperature by

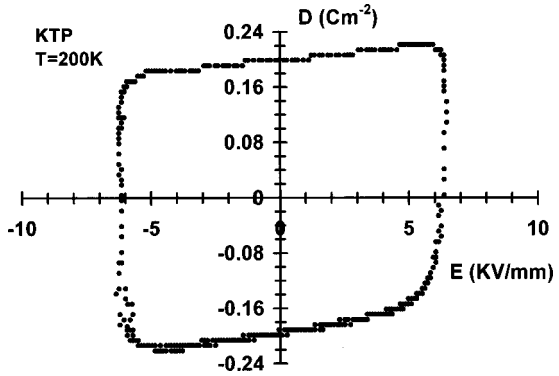

FIG. 7. The ferroelectric hysteresis loop of KTP at 200 K measured using the method of Ref. 31.

$$\sigma = \frac{\sigma_0}{T} e^{(2.4x10^{-5}E^{1/2} - E_a)/K_B T}. \tag{10}$$

To reduce the dc conductivity through decreasing the temperature, the condition required is $2.4\times10^{-5}E^{1/2}-E_a<0$. When $E_a=0.40$ eV, we have $E<277$ kV/mm. Under the electric field of up to 12 kV/mm required for domain inversion, this condition is well-satisfied so that decreasing the temperature is highly effective in decreasing the dc conductivity while a high electric field is applied.

E. Domain switching

Figure 7 shows a distorted hysteresis loop of KTP at 200 K, the compensation for which was selected large enough that the part of curve that crosses the *Y*-axis is linear. The rounded ends result from a conduction current density ($\sim$10 A m^{-2}) at high electric field, which cannot be removed by a linear compensation, i.e., the compensation voltage is proportional to the applied voltage.[31] Edged ends were observed at 170 K by Rosenman in ionically conducting KTP with the measured remanent polarization larger than the measured spontaneous polarization.[3,31] An ideal hysteresis loop was also observed by him using high-potassium-concentration KTP (Ref. 36) which is a low-conductivity material. Figure 7 shows that the remanent polarization at 200 K is 0.200 $\pm$0.005 C m^{-2}, which is larger than that at room temperature,[37] as expected.

A series of switching current density peaks for KTP at 200 K is shown in Fig. 8. These indicate that there is a difference between the coercive electric fields for the two senses of field application, i.e., along $+\mathbf{c}$ and $-\mathbf{c}$, as was also observed by Rosenman.[35] Furthermore, in a given sense of application, the coercive electric field changes with the number of inversions (e.g., the first and the third peak in Fig. 8). This behavior is most likely related to the redistribution of the vacancies in the crystal over time. A similar annealing effect was observed in x-ray diffraction studies of KTP under an electric field by Hamichi *et al.*[38]

The dependence of the coercive electric field on temperature is shown in Fig. 9. The coercive electric field increases as the temperature decreases, as expected. It is evident that domain switching can be realized at temperatures well above the superionic phase transition, if this is assumed to occur at 170 K. Therefore, the onset of ferroelectric switching behavior does not require either ''freezing in'' of the ions or a superionic phase transition.[3]

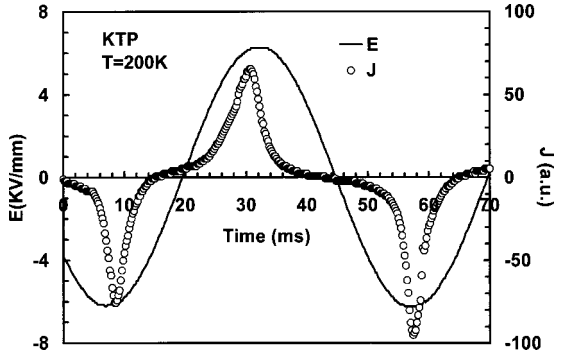

FIG. 8. Switching current peaks during the ferroelectric inversion of KTP at low temperature.

V. CONCLUSION

Flux-grown KTP undergoes three abnormal changes of its properties between room temperature and 140 K: (1) an order–disorder transition at 285 K, which accelerates the decrease of conductivity with temperature; (2) a superionic phase transition at 170 K, which is accompanied by an absorption of heat and an abnormal change in the thermal expansion; (3) a phase transition with an abnormal increase of spontaneous polarization and absorption of heat. The decrease in the thermal hopping frequency with decreasing temperature causes the variation in the frequency dispersion of both dielectric properties and conducting properties. Furthermore, the decrease of hopping frequency with temperature enables the transition from ionic conduction to electronic conduction to be observed at different temperatures for different frequencies. Decreasing temperature allows KTP to be ferroelectrically switched for the fabrication of QPM devices below 250 K.

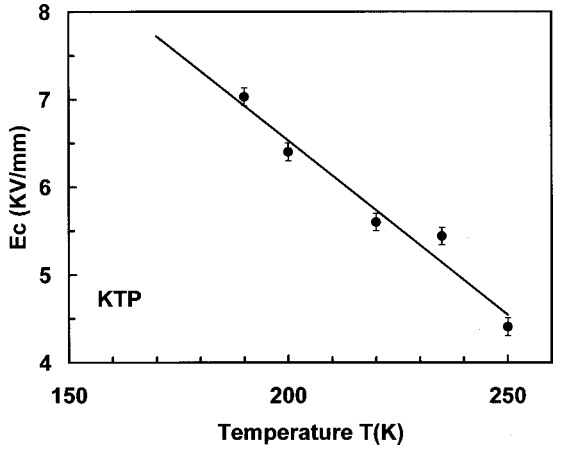

FIG. 9. Coercive electric field E_c as a function of temperature. The error bars show the error in the coercive electric field due to instrumental resolution. The line is the best fitting to the measured data points.

[1] J. D. Bierlein and H. V. Onherzeele, J. Opt. Soc. Am. B **6**, 622 (1989).
[2] H. Karlsson and F. Laurell, Appl. Phys. Lett. **71**, 3474 (1999).
[3] G. Rosenman, A. Skliar, D. Eger, M. Oron, and M. Katz, Appl. Phys. Lett. **73**, 3650 (1998).
[4] Q. Jiang, P. A. Thomas, K. B. Hutton, and R. C. C. Ward, ''Fabrication of periodically-poled $KTiOPO_4$ (KTP) isomorphs for nonlinear frequency conversion: Progress, problems, and solution,'' 15th Quantum Electrons and Photonics, 3–6 September 2001, Glasgow.
[5] D. T. Reid, G. T. Kennedy, A. Miller, M. Sibbett, and M. Ebrahimzadeh, IEEE J. Sel. Top. Quantum Electron. **4**, 238 (1998).
[6] P. A. Thomas and A. M. Glazer, J. Appl. Crystallogr. **24**, 968 (1992).
[7] P. A. Thomas, Q. Jiang, T. Latham, K. B. Hutton, and R. C. C. Ward, *Ferroelectrics 2000 UK*, edited by N. McAlford and E. Yeatman (Puto. IOM (Communication Ltd.), London, 2000), pp. 181–188.
[8] G. Rosenman, A. Skliar, M. Oron, and M. Katz, J. Phys. D **30**, 277 (1997).
[9] K. Nova, W. Sakamoto, T. Yogo, and S. Hirano, J. Mater. Sci. Lett. **19**, 69 (2000).
[10] V. A. Kalesinkskas, N. I. Pavlova, I. S. Rez, and J. P. Grigas, Lith. J. Phys. **22**, 87 (1982).
[11] J. Mangin, G. Jeandel, and G. Marnier, Phys. Status Solidi A **117**, 319 (1990).
[12] Yu. V. Shaldin and R. Poprawski, J. Phys. Chem. Solids **51**, 101 (1990).
[13] R. V. Pisarev, S. A. Kizhaev, J. P. Jamet, and J. Ferre, Solid State Commun. **72**, 155 (1989).
[14] A. U. Sheleg, E. M. Zub, L. A. Stremoukhova, and S. A. Guretskii, Crystallogr. Rep. **45**, 215 (2000).
[15] J. K. Han, D. K. Oh, C. H. Lee, C. E. Lee, J. N. Kim, and S. C. Kim, Phys. Rev. B **55**, 2687 (1997).
[16] K. S. Jim, E. R. Park, C. H. Lee, D. K. Oh, and C. E. Lee, Phys. Rev. B **64**, 132409 (2001).
[17] C. S. Tu, R. S. Katiyar, V. H. Schmidt, R. Guo, and A. S. Bhalla, Phys. Rev. B **59**, 251 (1999).
[18] Y. Yang and C. S. Yoon, Appl. Phys. Lett. **75**, 1164 (1999).
[19] M. Dammak, H. Khemakhem, N. Zouari, A. W. Kolsi, and T. Mhiri, Solid State Ionics **127**, 125 (2000).
[20] A. Haznar, A. Pietraszko, and I. P. Studenyak, Solid State Ionics **119**, 31 (1999).
[21] I. M. Bolesta, O. V. Futey, and O. G. Syrbu, Solid State Ionics **119**, 103 (1999).
[22] S. Geller, *Solid Electrolytes/Topics in Appl. Phys.* (Springer-Verlag, Berlin, Heidelberg, 1977).
[23] K. S. Cole and R. H. Cole, J. Chem. Phys. **9**, 341 (1941).
[24] A. K. Jonscher, *Universal Relaxation Law* (Chelsea Dielectric Press, London, 1996).
[25] T. Ishii, Prog. Theor. Phys. **73**, 1084 (1985).
[26] J. C. Kimball and L. Adams, Jr., Phys. Rev. B **18**, 5851 (1978).
[27] S. Alexander, J. Bernasconi, W. R. Schneider, and R. Orbach, Rev. Mod. Phys. **53**, 175 (1981).
[28] K. B. Hutton, R. C. C. Ward, and W. Godfrey, Mater. Res. Soc. Symp. Proc. **329**, 23 (1994).
[29] R. Helsel, *A Tutorial for HP-Vee* (Prentice–Hall, Englewood Cliffs, 1994).
[30] M. N. Womersley and P. A. Thomas, J. Appl. Crystallogr. **29**, 574 (1996).
[31] Q. Jiang, A. Lovejoy, P. A. Thomas, K. B. Hutton, and R. C. C. Ward, J. Phys. D: Appl. Phys. **33**, 1 (2000).
[32] J. Bernasconi, W. R. Schneider, and W. Wyss, Z. Phys. B **36**, 263 (1980).
[33] P. Urenski, N. Gorbatov, and G. Rosenman, J. Appl. Phys. **89**, 1850 (2001).
[34] P. Urenski, G. Rosenman, and M. Moloskii, J. Mater. Res. **16**, 1493 (2001).
[35] J. Frenkel, Phys. Rev. **54**, 647 (1938).
[36] G. Rosenman, P. Urenski, M. Roth, N. Angert, A. Skliar, and M. Tseitlin, Appl. Phys. Lett. **76**, 3798 (2000).
[37] G. D. Mahan, Phys. Rev. B **14**, 4345 (1976).
[38] M. Hamichi, R. Kariotis, and J. A. Venables, Phys. Rev. B **43**, 3208 (1991).